

Vibration Analysis of Ship Structures in Consideration of Fluid-Structure Interaction

Kie-Tae Chung ^{*}, Young-Bok Kim [†], Hyoung-Chol Shin [‡],
Sung-Ryong Han [§] and Young-Chol Huh [¶]

(From T.S.N.A.K., Vol. 29, No. 1, 1992)

Abstract

In the vibration analysis of today's weight-optimized ship structures, it is very easy to find the non-beam like modes of vibration such as the double bottom vibration or the local vibration in ships with large openings. However, it is not easy to find the added mass and the corresponding three dimensional reduction factors. It is well known that the hydroelastic vibration analysis of structures in contact with fluid can be solved by applying the finite element method to structures and the boundary element method to fluid domain. However, such an approach is impractical due to the characteristics of the fluid added mass matrix fully coupled on the whole wetted surface. To overcome this difficulty, an efficient program MOFSIA (Modal Fluid-Structure Interaction Analysis) based on the modal coupling of fluid-structure interaction using reanalysis scheme is developed for the free and forced vibration analysis of the arbitrary wetted structures with various fluid boundary conditions such as side wall, sea bottom or dock bottom, free surface and radiating boundary.

The efficiency and accuracy of calculated results using the program MOFSIA developed by this project has been proved through the vibration experimental measurements of the plate model and the ship model, and also through the numerical experiments for the same models and 3200 TEU container ship.

1 Introduction

It is the trend that the ship is constructed as more and more light weight-optimized with growing power. Therefore, the control of the ship vibration is becoming important problem

^{*}Member, Department of Naval Architecture and Ocean Engineering, Chungnam National University

[†]Member, R & D Center, Korean Register of Shipping

[‡]Member, Department of Naval Architecture and Ocean Engineering, Seoul National University

[§]Member, Ship and Marine Institute, Samsung Heavy Industry Ltd.

[¶]Member, Ship and Marine Institute, Samsung Heavy Industry Ltd.

from the early stage in the ship design. Nevertheless, the lighter the ship constructed with higher power, the severer the vibration of the ship becomes. In most cases the ship vibration shows the combined modes between the hull girder modes and the local vibration modes.

In reference[5] Chung, et. al., has proposed a new effective analysis method to solve such a complicate global-local mixed mode vibrations considering the fluid-structure interaction problems as a whole.

In this paper as a next step of the former paper [5], the additional developments are performed in order to solve fluid-structure interaction problem with more complicate fluid boundaries such as sea bottom, side wall, radiation boundary. For this purpose, the Green's function expansions satisfying the boundary conditions are taken as a weighting function in the general weighted residual formulation.

2 Theory

2.1 Boundry-Value Problem

The surrounding water of vibrating structure is assumed as an ideal fluid and the velocity potential $\Phi(\xi; t)$ is separated in case of the fluid-structure interaction problem as follows;

$$\Phi(\xi; t) = Re\{\phi(\xi)e^{i\omega t}\} \quad (1)$$

where $\phi(\xi)$ is the function of spatial coordinate ξ . If the structure is vibrating in fluid, the boundary value problem can be defined as follows[2,5];

Governing equation :

$$\nabla^2 \phi = 0 \quad on \quad \Omega_F \quad (2)$$

Boundary conditions :

$$\frac{\partial \phi}{\partial n} = G^T \dot{W} \quad on \quad \Gamma_S \quad (3)$$

$$\phi = 0 \quad on \quad \Gamma_F \quad (4)$$

$$\frac{\partial \phi}{\partial n} = 0 \quad on \quad \Gamma_B \quad (5)$$

$$\frac{\partial \phi}{\partial n} = ik\phi \quad on \quad \Gamma_R \quad (6)$$

where G^T is the transformation matrix from structural DOF's to fluid vector components at any node normal to the wetted structural surface, \dot{W} is the structural velocity, k is wave number and Γ_S , Γ_F , Γ_B , Γ_R are the fluid boundaries on the wetted structural surface, free surface, bottom or side wall and radiation surface, respectively. The equations of motion representing a fluid-structure interaction can be described as follows:

2.1.1 The Boundary Integration

To solve the Boundary Value Problem(BVP) composed of the governing equation (2) and the boundary conditions (3) (6), the generalized weighted residual integral by introducing the weighting function ϕ^* to the BVP is obtained as follows[2];

$$\int_{\Omega_F} \nabla^2 \phi \phi^* d\Omega = \int_{\Gamma_S} \left(\frac{\partial \phi}{\partial n} - G^T \dot{W} \right) \phi^* d\Gamma + \int_{\Gamma_R + \Gamma_F} \phi \phi^* d\Gamma + \int_{\Gamma_B} \frac{\partial \phi}{\partial n} \phi^* d\Gamma \quad (7)$$

As explained in [2], the inverse formulation can be obtained by integrating the equation (7) partially twice as follows;

$$\begin{aligned} \int_{\Omega_F} \nabla^2 \phi^* \phi d\Omega = & - \int_{\Gamma_F + \Gamma_R} \nabla \phi \phi^* d\Gamma + \int_{\Gamma_S + \Gamma_B} \frac{\partial \phi^*}{\partial n} \phi d\Gamma \\ & - \int_{\Gamma_S} G^T \dot{W} \phi^* d\Gamma + \int_{\Gamma_R + \Gamma_F} \phi \phi^* d\Gamma \end{aligned} \quad (8)$$

In order to obtain the boundary integral formulations, the weighting function ϕ^* should be taken as Green's function to satisfy the governing equation (2). Therefore, the Green's function satisfies the following equation ;

$$\nabla^2 \phi^*(\xi; x) = \delta(\xi - x) \quad (9)$$

By substituting (9) into the left-hand side of equation (8),

$$\begin{aligned} c(x)\phi(x) - \int_{\Gamma_F + \Gamma_R} \nabla \phi \phi^* d\Gamma + \int_{\Gamma_S + \Gamma_B} \frac{\partial \phi^*}{\partial n} \phi d\Gamma \\ + \int_{\Gamma_R + \Gamma_F} \phi \phi^* d\Gamma = \int_{\Gamma_S} G^T W(x) \phi^* d\Gamma \end{aligned} \quad (10)$$

where $c(x)$ is the form factor depending on the configuration of the wetted structural surface. The fundamental solutions of equation (9) for 3-D and 2-D satisfying only governing equation (2) are as follows[2] ;

$$\phi^*(\xi; x) = \frac{1}{4\pi r(\xi; x)} \quad \text{for} \quad 3 - D \quad (11)$$

$$\phi^*(\xi; x) = \frac{1}{2\pi} \ln \frac{1}{r(\xi; x)} \quad \text{for} \quad 2 - D \quad (12)$$

where ξ and x denote the source point and observation point, respectively, and $r(\xi; x) = |\xi - x|$. Finally, equation (10) is the fundamental equation for the boundary integration performed to solve the BVP of fluid domain. According to selecting the Green's function satisfying the boundary conditions in (3)-(6), the boundary integration formulation can be obtained simpler as explained in the following 4 cases.

(1) Fully-submerged Structure

In this case the boundary conditions except (3) and (6) are automatically satisfied at infinite long distance $r \rightarrow \infty$ from the structure. Therefore, the equation (10) can be

rewritten by inserting the Green's functions (11) or (12) as follows;

$$c(x)\phi(x) + \int_{\Gamma_S} \frac{\partial \phi^*}{\partial n} \phi d\Gamma = \int_{\Gamma_S} G^T W(x) \phi^* d\Gamma \quad (13)$$

(2) Free Surface Effect

Green's functions are taken to satisfy the two boundary conditions, which are the radiating boundary condition on the radiating surface at infinite water depth and free surface boundary condition in equation (4). And now this problem can be redefined as a BVP in half infinite fluid domain. In this case the radiating condition can be automatically satisfied. In order to satisfy $\phi = 0$ on Γ_F , the Green's function can be taken using the mirror effect as follows;

$$\phi^*(\xi; x) = \phi^*(\xi^0; x) - \phi^*(\xi^1; x) \quad (14)$$

where $\xi^0 = \xi$, $\xi^1 = -\xi$ are shown in Fig. 2.

(3) Shallow Water Effect

When the fluid boundaries are bounded by the free surface and sea bottom, the Green's function satisfying the two boundary conditions can be obtained as the infinite series expansions of Green's functions continuously reflected by the two parallel bounding surfaces as follows;

$$\phi^*(\xi; x) = \phi^*(x^0; x) - \phi^*(\xi^1; x) + \sum -1^n (\phi_2 n^* - \phi_3 n^* + \phi_4 n^* - \phi_5 n^*) \quad (15)$$

where $\phi_k n^* = \phi_k n^*(\xi^k; x)$ and ξ^k are the coordinates of the k -th reflected image sources as shown in Fig. 3.

(4) Side Wall Effect

When the fluid is bounded by all boundaries such as free surface, bottom and side wall can be handled as in the same way in case (3), so that the combined form of equation (13), (14) and (15) is obtained as follows;

$$\begin{aligned} \phi^*(\xi; x) = & \phi^*(\xi^0; x) - \phi^*(\xi^1; x) + \sum (-1)^n (\phi_2 n^* - \phi_3 n^* + \phi_4 n^* - \phi_5 n^*) + \\ & \phi^*(\xi^6; -x) - \phi^*(\xi^7; -x) + \sum (-1)^n (\phi_8 n^* - \phi_9 n^* + \phi_{10} n^* - \phi_{11} n^*) \end{aligned} \quad (16)$$

where ϕ_n^* are shown in Fig. 4 and $\xi^{i+6} = \xi^i (i = 0 - 6)$.

2.2 Boundary Element Method

By taking the various Green's function in (11), (12) and (14) (16) according to the fluid boundary configurations, the boundary integral equation (13) can be obtained and solved

easily as explained in [2]. After solving this equation we can get the nodal pressure as a function of normal structural velocity.

$$P_I(x, t) = \rho A_m(x) G^T \ddot{W}(x, t) \quad (17)$$

The integration of the pressure over the structural surface gives total added inertia force due to fluid-structure interaction as follows;

$$F_I(x, t) = -M_F G^T \ddot{W}(x, t) \quad (18)$$

$$M_F = \rho \int_{\Gamma_S} \bar{n}(s) N(s) d\Gamma(s) A_m(x) \quad (19)$$

where $N(s)$ represents approximating function for the structural surface. M_F is fluid added mass matrix, which is asymmetric and fully coupled due to the characteristics of the Green's function, that is, $N(s)$ and Green's function are different. The following equation is representing the motion of equation for fluid-structure interaction.

$$M_S \ddot{W} + C_S \dot{W} + K_S W = F_E + F_I \quad (20)$$

where, M_S = mass matrix of structure C_S = damping matrix of structure F_E = pure external force F_I = inertia force on the wetted surface due to fluid-structure interaction

The analysis for fluid-structure interaction means the problem to obtain F_I as a function of the structural response function. Since the fluid is taken as ideal, the tangential force is ignored. Then, substituting equation (18) into equation (20),

$$(M_S + M_F) \ddot{W} + C_S \dot{W} + K_S W = F_E \quad (21)$$

2.3 Free and Forced Vibration

Chung, et. al., have proposed an effective fluid-structure interaction analysis method using modal reanalysis in [5]. The general formulation for the vibration problem of the wetted structure is described in equation (21). When the exciting forces are given and the structural damping matrix is defined in the form of proportional damping or structural damping, the forced response at any structural node can be easily calculated by mode superposition method.

3 Experiments and Numerical Analyses

3.1 Circular Plate with Clamped Edge Boundary Condition

The plate is selected as the model referred in [8,9] for studying the free surface effect and bottom effect (shallow water effect) of a circular plate, of which the dimension is $d \times h = 600\phi \times 3.1mm$ and the boundary edges are all clamped[6]. The results of measurement and calculation are summarized in Table 1. For the circular plate submerged near the free surface, the experiments reveal that the natural frequencies of diametrical modes of circular plate are well coincident with calculations. Some discrepancies in circular modes are supposed to occur from the uncertainty of supporting structure which realizes the clamped boundary condition.

3.2 Cantilever Vertical Surface-piercing Rectangular Plate

The reference is made to [10,11] for this model. The dimension of plate is $a \times b \times h = 1000 \times 400 \times 5.2\text{mm}$ [6]. The experimental results are well in accordance with the results calculated by the proposed method upto the first two mode (0,0), (1,0), but includes some errors of 9-13 consistence with the calculated results, except the cases that are located very close to side wall, as summarized in Table 2.

3.3 Ship Model

The open top container was adopted as a mother ship for a model, since she is expected to exhibit the phenomena of the hull girder-local coupled vibration and horizontal/torsional coupled vibration. The similarity for principal dimension is kept to see the coupling effect of the hull girder with the plate local vibration in high order vibration mode. In addition, two removable bulkheads were installed to review the problem of the hull girder-local coupled vibration.

3.3.1 Model Characteristics

Principal Dimensions :

L. O. A. = 2.75 *m*

Breadth = 0.31 *m*

Depth = 0.16 *m*

Hold Length = 0.25 *m*

Draft (Estimated) = 0.1014 *m*

(Measured) = 0.1000 *m*

No. of Hold = 8

Young's Modulus = 1.960E+11 *N/m²*

Poisson's Ratio = 0.3

Density = 7.850E+03 *kg/m³*

Plate Thickness = 3.2 *mm*

Weigh (Estimated) = 68.94 *kg*

(Measured) = 67.50 *kg*

The installation of side stringer, transverse web frame and removable bulkhead specially designed were considered for the model to distinguish the hull girder vibration and the plate local vibration from the coupling phenomena.

3.3.2 Results of Experiments and Numerical Analyses

(1) Effect of Removal of Bulkhead

Removal of bulkhead causes to increase the natural frequency due to reducing bulkhead mass in the sense of global vibration, and remarkably to decrease the natural frequencies

of platings. Accordingly, the addition of side shell and bottom plate have the effect on the global natural frequency over three modes. For the case of bulkhead removed, natural frequencies are generally increased at each mode. On the contrary, the removal of two bulkheads has made the 3rd mode natural frequency of horizontal/torsional vibration to be decreased as much as 4.2 compared to that in air and the 2nd and the 3rd mode natural frequencies of vertical vibration and the 3rd mode natural frequency of horizontal/torsional vibration to be decreased as much as 3.1 6.3 plate local vibration.

(2) Shallow Water Effect

The distance c apart from bottom and side wall are shown in Fig. 5, where c was determined to be 70 cm as much as 7 times the draft to exclude any other effect. The distance h above bottom started at 70 cm and tested as decreasing as much as 5 cm stepwisely. When h/d became 5.0, the bottom effect was shown up, and when the ratio came down to 3.0 in vertical mode and 2.0 in horizontal/torsional mode, the bottom effects were remarkable. The results of measurement and calculation are summarized in Table 3 and shown in Fig. 6-1 and 6-2.

(3) Wall Effect

While the distance h was retained as 70 cm, the distance c was varied from 70 cm to 1 cm. The wall effect has been shown up gradually at $c/d=2.0$, and it became severely to appear at below $c/d=0.5$ in vertical vibration and at below $c/d=0.1$ in horizontal/torsional vibration. According to the variation of distance from wall, the results are summarized in Table 4 and shown in Fig. 7-1 and 7-2. In Fig. 7-1, the calculated natural frequencies of the 3rd vertical mode show larger discrepancies from the measured ones. It is due to the fact that it was very difficult to distinguish the correct modes in experiments. The smaller the distance c is, the larger the differences of frequencies become.

(4) Fluid Model Size

The effect of fluid model size on the natural frequencies is studied as presented in Table 5 and Fig. 8. These show that the results obtained with the largest fluid model can be also made even with the one-quarter smaller fluid model without losing significant accuracy.

3.4 Measurement and Analyses for SHI 3200 TEU Container

3.4.1 Free Vibration

A container vessel which has been newly built by SHI designated as HN 1102 and $L \times B \times D = 224.0 \times 32.2 \times 19.1m$ was selected for application. The measurements have been carried out during exciter test in dock side. Also, the analysis has been carried out in all the following loading and test conditions.

The comparisons of the natural frequencies among the calculated ones by VMM of

Draft	Aft Draft	Forward Draft
Exciter test	6.0 m	0.6 m
Ballast	8.31 m	2.80 m
Full load	10.993 m	10.589 m

NASTRAN, those by the proposed method and the measurement are listed in Table 6. This table shows the natural frequencies by NASTRAN and the proposed method have approximately same accuracy. But the main advantages of the proposed method is the fairly small DOF's to be required in modelling in order to solve the complicated BVP involving the boundary conditions on the sea bottom, the dock side wall and the far field radiation surface. Therefore, the data required for the vibration analysis of ship, for example, of exciter test condition at dock side can be prepared much simpler than that of NASTRAN.

4 Conclusion

In order to improve the direct fluid-structure coupling vibration analysis method based on the modal reanalysis scheme proposed in [5], the Green's function expansions satisfying the boundary conditions on the free surface, bottom, side wall and radiation surface are implemented in the generalized weighted residual integration. The experiments to measure the natural frequencies of the clamped circular plate and the cantilevered vertical surface-piercing plate were carried out to verify the accuracy of the proposed method. In the experiment of ship model, the other one of the efficiencies of this proposed method is proved through the study that the analysis result with the fluid model of one-quarter size of structure was as good as that with the fluid model of full size structure. From the comparisons of the natural frequencies of experiments in exciter test at dock side with those of calculations by NASTRAN VMM and the proposed method for 3200 TEU container, it is shown that the accuracy and effectiveness of the proposed method are fairly satisfactory. The main advantages of the proposed method is the fairly small DOF's to be required in modelling in order to solve the complicated BVP. Therefore, the data required for the vibration analysis of ship with complicated fluid boundaries can be prepared much simpler than that of NASTRAN.

References

- [1] Zienkiewicz, O. C. and Bettles, P., "Fluid-Structure Dynamic Interaction and Wave Forces," *An Introduction to Numerical Treatment, Numerical Methods in Engineering*, Vol. 13, 1978, pp.1-16.

- [2] Chung, K.T., "On the Vibration of the Floating Elastic Body Using Boundary Integral Method in Combination with Finite Element Method," *Journal of the Society of Naval Architects of Korea*, Vol. 24, No. 4, 1987.
- [3] Hakala, M.K. and Matusiak, J., "A Practical Approach for the Estimation and Verification of Ship Vibration Response," The 2nd Int'l. Symp. on Practical Design in Shipbuilding, PRADS 83, Tokyo & Seoul, 1983.
- [4] Wang, B.P., "Reanalysis of Structural Dynamic Models," *American Society of Mechanical Engineers*, AMD - Vol. 76, 1986.
- [5] Chung, K.T., Kim, Y. B., Kang, H. S., "Hydroelastic Vibration Analysis of Structures in contact with Fluid," PRADS 92, Newcastle Upon Tyne, G.B., 1992. 5.
- [6] Shin, H. C., "Experimental Study on the Vibration of Clamped Circular Plate and Cantilevered Vertical Surface-piercing Rectangular Plates in Contact with Water", Master Thesis, Seoul National University, 1993.
- [7] Petyt, M., Introduction to Finite Element Vibration Analysis, Cambridge University Press, 1991.
- [8] Lindholm, U. S., Kana, D. D., Chu, W. H. and Abramson, H. N., Elastic Vibration Characteristics of Cantilever Plates in Water, *Journal of Ship of Applied Mechanics*, Vol. 58, No. 2, 1992.
- [9] Marcus, M. S., A Finite Element Method Applied to the Vibration of Submerged Plates, *Journal of Ship Research*, Vol. 22, No. 2, SNAME, 1978.
- [10] Lindholm, U. S., Kana, D. D., Chu, W. H. and Abramson, H. N., "Elastic Vibration Characteristics of Cantilever Plates in Water", *Journal of Ship Research*, Vol. 9, No. 1, SNAME, June, 1965.
- [11] Marcus, M. S., "A Finite Element Method Applied to the Vibration of Submerged Plates", *Journal of Ship Research*, Vol. 22, No. 2, SNAME, 1978.
- [12] Kim, Y. B., "Vibration Analysis of Plates in Contact with Water by the FE-BE Method", Master Thesis, Seoul National University, 1994.

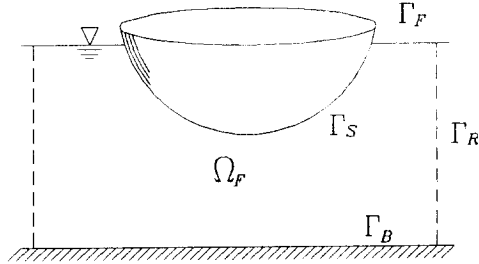


Figure 1: Definition of domain and boundaries[12]

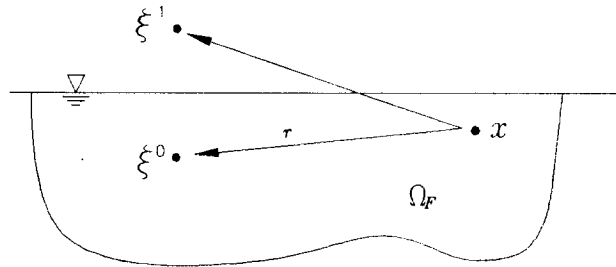


Figure 2: Image source(\$\xi^1\$) by free surface[12]

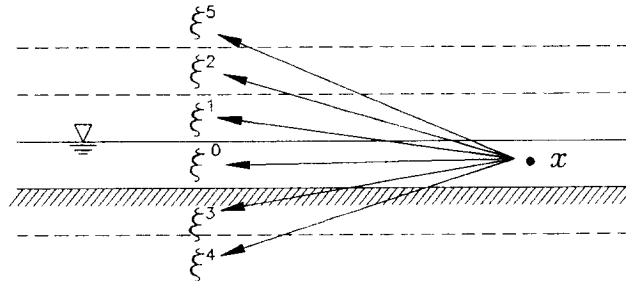


Figure 3: Image sources of series from(\$\xi^k\$) by free surface and bottom[12]

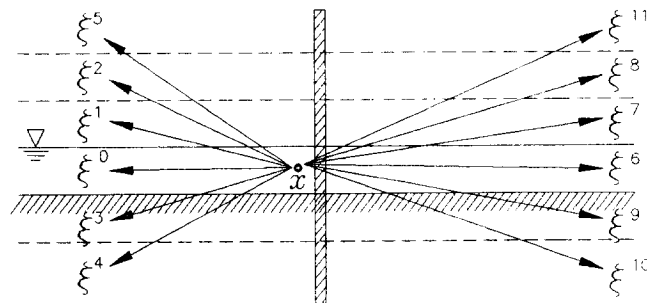


Figure 4: Image sources of series from(\$\xi^k\$) by free surface, bottom and side wall[12]

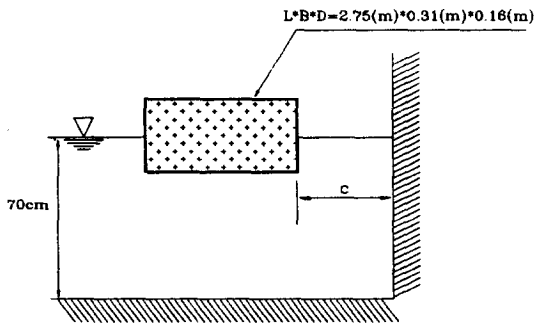


Figure 5: Ship mode in small basin

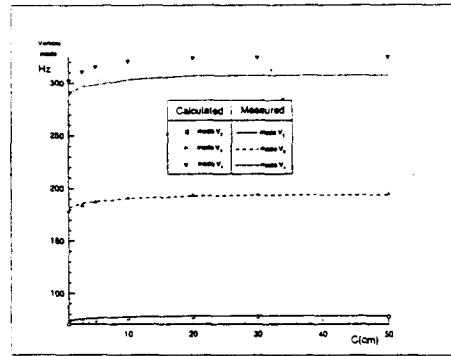


Figure 7-1: Side wall effects on the natural frequencies of horizontal/torsional modes for ship model

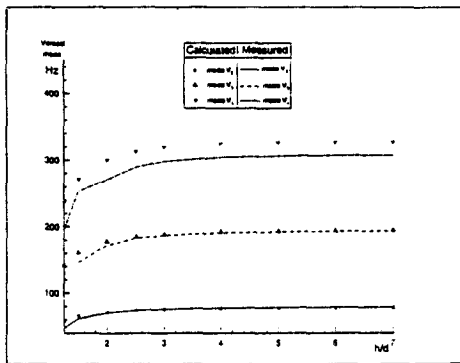


Figure 6-1: Shallow water effects on the natural frequencies of vertical modes for ship model

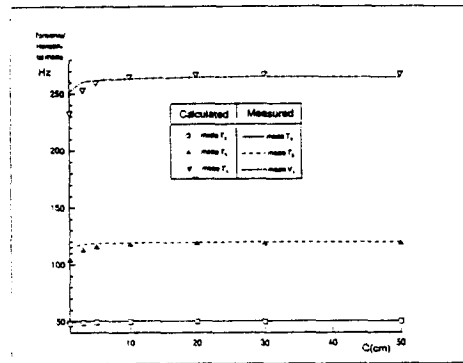


Figure 7-2: Side wall effects on the natural frequencies of vertical modes for ship model

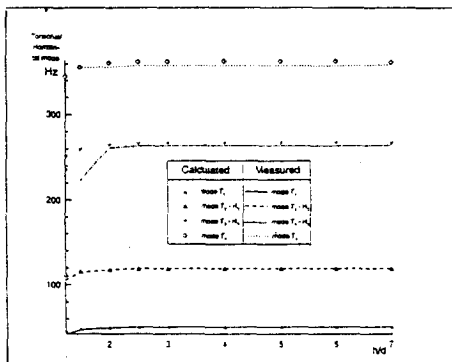


Figure 6-2: Shallow water effects on the natural frequencies of horizontal/torsional modes for ship model

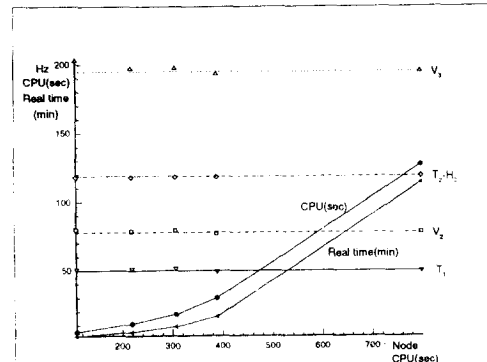


Figure 8: Comparison of user times, CPU times and natural frequencies of ship model coupled with various fluid models

Table 1: The effects of water and free surface of clamped plate

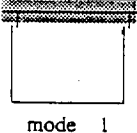
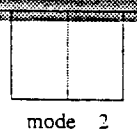
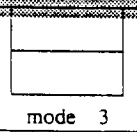
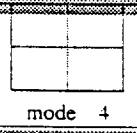
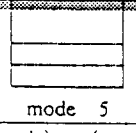
[Hz]

air/water mode (m,n)	in air	depth of water in fluid : d (cm)													
		0.0	2.5	4.0	6.0	9.0	12.0	15.0	18.0	21.0	25.0	30.0	35.0	40.0	
(0,0)	MEASURE**	84.5(84.7)*	26.3	25.1	24.8	23.8	22.9	22.3	21.7	21.7	21.2	20.8	20.6	20.6	
	MOFSIA	84.7	26.4	43.9	36.6	31.2	26.7	24.3	22.7	21.7	21.0	20.3	19.8	19.4	19.2
(1,0)	MEASURE**	173.2(176.2)*	78.6	72.1	71.3	68.3	64.1	62.6	60.4	60.3	60.2	60.2	59.9	59.9	59.9
	MOFSIA	176.2	78.1	100.1	85.5	75.0	67.3	63.5	61.5	60.3	59.6	59.0	58.6	58.3	58.2
(2,0)	MEASURE**	283.9(289.1)*	148.1	123.8	121.4	116.9	114.8	114.6	114.2	113.7	113.2	—	—	—	113.2
	MOFSIA	289.0	148.6	168.0	145.7	130.1	121.0	117.0	115.1	114.2	113.6	113.2	113.0	112.8	112.7
(0,1)	MEASURE**	328.3(329.7)*	173.8	138.0	136.0	132.2	130.1	129.0	128.6	128.6	—	—	—	—	128.6
	MOFSIA	328.8	146.8	170.2	145.8	130.4	120.5	116.3	114.1	112.8	111.9	111.0	110.3	109.8	109.4
(3,0)	MEASURE**	415.6(423.1)*	229.3	215.9	204.3	192.1	187.6	185.8	185.3	185.3	—	—	—	—	185.3
	MOFSIA	424.5	231.5	250.5	220.7	202.3	191.7	187.9	186.4	185.6	185.2	184.9	184.6	184.4	184.3
(1,1)	MEASURE**	493.2(504.2)*	296.9	250.3	244.7	234.7	229.7	226.9	226.9	—	—	—	—	—	226.9
	MOFSIA	502.7	275.4	255.6	251.9	232.4	221.4	217.2	215.2	214.0	213.2	212.4	211.9	211.5	211.2

Remark) () * : Theory , ** : Measured[6,12]

Table 2: Natural frequencies of measured and calculated cantilevered piercing plate subjected to wall effects[6,12]

[Hz]

modes	c(cm)	s/a	0.2	0.4	0.6	0.8	1.0																
 mode 1	50	40	20	10	4	2.9 (2.96)	3.0 (2.96)	3.0 (2.92)	2.8 (2.94)	2.8 (2.91)	2.1 (2.25)	2.2 (2.25)	1.8 (1.98)	1.7 (1.87)	1.7 (1.87)	1.7 (1.83)	1.7 (1.82)	1.6 (1.79)	1.5 (1.74)	1.3 (1.68)			
	 mode 2	50	40	20	10	4	18.5 (17.88)	18.5 (17.88)	18.4 (17.87)	18.4 (17.82)	18.0 (17.65)	14.9 (14.68)	14.8 (14.67)	13.5 (13.26)	13.4 (13.25)	12.9 (12.73)	12.9 (12.6)	12.9 (12.6)	12.8 (12.5)	12.5 (12.3)	11.7(11.99)		
		 mode 3	50	40	20	10	4	23.0 (23.68)	22.9 (23.68)	22.9 (23.67)	22.8 (23.64)	22.6 (23.59)	19.7 (21.53)	19.7 (21.52)	14.1 (16.56)	14.1 (16.55)	11.5 (13.87)	11.5 (13.87)	11.4 (13.82)	10.7 (13.68)	9.90 (12.9)	8.70 (12.6)	
			 mode 4	50	40	20	10	4	66.6 (62.47)	66.6 (62.47)	66.5 (62.45)	66.4 (62.37)	66.0 (62.13)	62.4 (60.43)	62.4 (60.43)	47.5 (50.76)	47.4 (50.76)	42.4 (43.82)	42.5 (43.81)	42.4 (43.71)	41.5 (43.33)	39.9 (40.5)	37.3 (39.4)
				 mode 5	50	40	20	10	4	77.9 (69.65)	77.8 (69.65)	77.8 (69.63)	77.3 (69.60)	77.2 (69.53)	75.2 (60.46)	70.6 (60.45)	49.6 (56.75)	49.7 (56.74)	36.5 (45.82)	36.6 (45.24)	36.2 (45.21)	34.9 (45.06)	29.4 (41.5)

Remark) () : MOFSIA

s/a : Immersion ratio of plate in water, c(cm) : distance from plate to wall

Table 3: The shallow water effect on the natural frequencies of the ship model

(c=80cm) [Hz]

		h/d	7.0	6.0	5.0	4.0	3.0	2.5	2.0	1.5	1.25	
Vertical Mode	V ₂	MEASURE	78.57	78.57	78.04	77.4	75.89	74.25	70.58	61.17	47.26	
		MOFSIA	77.9	77.59	77.32	76.75	75.35	73.89	71.17	65.14	58.28	
	V ₃	MEASURE	193.84	193.75	192.40	191.14	187.09	182.59	172.28	146.02	—	
		MOFSIA	194.9	194.38	193.83	192.50	189.10	185.24	177.9	161.2	142.10	
	V ₄	MEASURE	307.65	307.5	306.36	304.41	297.75	289.46	270.49	252.34	195.64	
		MOFSIA	327.0	326.54	325.92	324.2	319.0	312.67	300.0	270.6	236.95	
	V ₅	MEASURE	—	—	—	—	—	—	—	—	—	
		MOFSIA	430.7	430.41	429.94	428.4	422.6	414.77	397.7	356.1	308.47	
	Torsional /Horizontal Mode	T ₁	MEASURE	50.40	50.40	50.32	50.34	50.25	50.11	49.62	47.44	42.33
			MOFSIA	49.92	49.92	49.91	49.89	49.81	49.68	49.31	47.91	45.34
T ₂ -H ₂		MEASURE	119.62	119.6	119.5	119.54	119.43	119.11	118.05	114.19	105.63	
		MOFSIA	118.73	118.73	118.71	118.66	118.47	118.18	117.40	115.01	111.27	
T ₃ -H ₃		MEASURE	264.56	263.75	264.07	264.18	264.0	263.31	261.14	222.06	—	
		MOFSIA	267.67	267.67	267.65	267.56	267.18	266.56	264.90	259.49	251.06	
T ₄		MEASURE	359.19	357.5	357.97	357.89	357.94	357.92	355.94	355.36	—	
		MOFSIA	363.04	363.03	363.02	362.98	362.77	362.29	361.10	355.78	345.04	

Remark) 325.52 Hz (h/d = 7.0) : V4 mode

Table 4: Results of measured and calculated natural frequencies by the effects of side wall on the ship model

[Hz]

Direc.	Mode shape	c(cm)	50	30	20	10	5	3	1
		results							
Vertical mode	V ₂	MEASURE	78.52	78.49	78.18	77.21	76.15	75.67	73.93
		MOFSIA	77.66	77.45	77.11	75.95	74.21	72.82	70.39
	V ₃	MEASURE	193.86	193.67	192.93	190.57	187.30	186.29	181.57
		MOFSIA	194.48	194.16	193.50	191.06	187.16	183.98	178.33
	V ₄	MEASURE	307.63	307.06	306.80	303.32	298.21	296.61	290.60
		MOFSIA	324.82	324.24	323.84	320.71	315.22	310.59	302.13
Torsional /Horizontal mode	T ₁	MEASURE	50.41	50.52	50.36	50.26	50.15	50.09	49.82
		MOFSIA	49.91	49.88	49.82	49.60	49.22	48.87	48.12
	T ₂	MEASURE	119.69	119.99	119.55	119.15	118.45	117.96	114.71
		MOFSIA	118.71	118.64	118.47	117.54	115.20	112.45	104.06
	T ₃	MEASURE	264.30	265.09	264.41	263.14	261.86	260.55	251.86
		MOFSIA	267.66	267.56	267.23	265.25	259.90	253.39	233.15

Table 5: The fluid model size effect on the natural frequencies of the model

Model		Model 1	Model 2	Model 3	Model 4	Model 5	
Model Size	Node	799	389	307	219	109	
	Element	236	112	84	60	30	
No. of elements per one hold in bottom		2 x 5	2 x 3	1 x 3	1 x 2	1 x 1	
No. of elements per one hold in shell		2 x 5	1 x 3	1 x 3	1 x 2	1 x 1	
Run Time	Real Time (H:M:S)	1:54:00	0:16:26	0:08:56	0:04:48	0:02:15	
	User Time (H:M:S)	1:51:25	0:15:51	0:08:36	0:04:34	0:02:08	
	CPU (M:S)	2:07	0:30	0:18	0:11	0:5	
Eigen-frequency (Hz)	Symmetry Mode	1st	77.89	77.13	78.98	78.72	79.83
		2nd	194.82	193.26	197.43	197.21	202.82
		3rd	325.04	323.55	329.17	328.37	349.99
		4th	427.70	428.49	434.06	420.47	489.04
		5th	665.55	668.75	703.43	683.73	663.66
	Anti-symmetry Mode	1st	49.92	49.48	51.36	51.19	50.90
		2nd	118.74	118.26	118.11	117.99	117.81
		3rd	267.68	266.93	266.45	266.46	266.95
		4th	363.04	363.46	371.02	371.65	371.69
		5th	462.84	462.64	462.30	463.07	468.36

Table 6: Results of calculated and measured natural frequencies for HN1102 (in the exciter test condition)

[Hz]

Mode	Calculated					MEASURE
	Proposed method				NASTRAN	
	10 modes	20 modes	30 modes	40 modes		
V_2	1.10	1.12	1.09	1.09	1.13	1.66
V_3	2.06	2.08	1.99	1.98	2.12	2.33
V_4	3.27	3.21	3.07	3.06	3.08	3.0
V_5	4.42	4.03	3.79	3.78	3.93	3.42